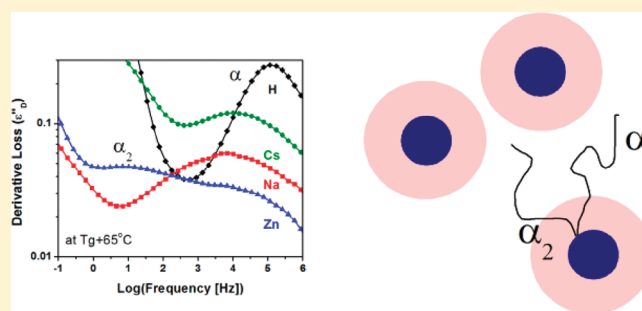


Influence of Cation Type on Structure and Dynamics in Sulfonated Polystyrene Ionomers

Alicia M. Castagna,[†] Wenqin Wang,^{‡,§} Karen I. Winey,^{*,‡} and James Runt^{*,†}[†]Department of Materials Science and Engineering, The Pennsylvania State University, University Park, Pennsylvania 16802, United States[‡]Department of Materials Science and Engineering, University of Pennsylvania, Philadelphia, Pennsylvania 19104, United States

S Supporting Information

ABSTRACT: The structure and dynamics of Na-, Cs-, and Zn-neutralized sulfonated polystyrene (SPS) ionomers were investigated using scanning transmission electron microscopy (STEM), X-ray scattering, and dielectric relaxation spectroscopy. Aggregates ~ 2 nm in diameter were revealed by STEM and X-ray scattering. Additional information on aggregate diameter, radius of closest approach, and number density were determined by fitting the scattering data with a modified hard sphere model. A single broad segmental relaxation was identified in dielectric loss spectra for the ionomers neutralized with monovalent ions Cs and Na. The relaxation time of the segmental process was found to slow down systematically with increasing degree of sulfonation but is not significantly affected by monovalent ion type. For Cs-neutralized SPS, two high temperature relaxations associated with Maxwell–Wagner–Sillars and ion association/dissociation dynamics were identified.



■ INTRODUCTION

Ionomers, polymers containing ionic functionality, have been a significant research focus over the past 5 decades.¹ Their enhanced properties, such as toughness and moduli, over their non-ionic counterparts make these materials attractive for a breadth of applications including performance coatings, films, adhesives, and tough thermoplastic parts.¹ This property enhancement arises from the microphase separation of ionic species into aggregates due to strong electrostatic interactions, which behave as thermoreversible cross-links.¹

Extensive investigation of the morphology of these ionic rich domains and resulting mechanical and dynamic mechanical properties of these materials has been performed.^{1–11} However, the fundamental connection between aggregate structure and molecular dynamics is not well-defined. Dielectric relaxation spectroscopy (DRS) is a powerful tool for probing molecular dynamics and can reveal information about segmental chain motion, ion motion and polarization processes.

In an effort to elucidate the correlation between ionic aggregate structure and dynamics, we systematically investigated a model ionomer, sulfonated polystyrene (SPS), with varying degrees of sulfonation and neutralization as well as neutralizing ion types, utilizing X-ray scattering, scanning transmission electron microscopy, and DRS. In two previous publications, we discussed the effect of sulfonation on the structure and dynamics of SPS acid copolymers and the influence of neutralizing these copolymers with zinc.^{12,13} In the current paper we examine the role of neutralizing ion type (Na, Cs, and Zn) and discuss the effects of sulfonation and neutralization on structure and dynamics of Cs- and Na-neutralized SPS.

■ EXPERIMENTAL SECTION

Sample Preparation. Atactic polystyrene, purchased from Pressure Chemical ($M_w = 123$ kg/mol, PDI = 1.06), was sulfonated according to a previously published procedure.¹² SPS acid copolymers were neutralized by dissolving in a 90/10 v/v mixture of toluene/methanol. A stoichiometric amount of metal acetate (Na, Cs, and Zn) was dissolved in a 50/50 v/v mixture of toluene/methanol and added slowly into the gently agitated SPS solution to achieve different percentages of neutralization. The reaction was held at 50 °C for 2 h. In this publication, the ionomers are designated as SPS x - y M, where x is the mole percent of sulfonation (3.5, 6.7, or 9.5), y is the percent neutralization (0, 25, 50, 75, and 100), and M is the neutralizing ion (Na, Cs, or Zn). In total, 23 polymers were studied and are listed in Table 1.

The neutralized ionomers were solvent cast at ambient conditions, air-dried for 1–2 days, and then dried under vacuum at 120 °C for at least 24 h. Ionomers with T_g around or above 120 °C (SPS6.7- y M and SPS9.5- y M) were further annealed at $\sim T_g + 20$ °C for another day. The dried ionomer films were then hot pressed at 160 °C and used for X-ray scattering, STEM imaging, and dielectric spectroscopy. All materials were stored in vacuum desiccators prior to characterization. Selected samples were sent to the Galbraith Laboratories for elemental analysis to determine the percent neutralization. The results were consistent with the stoichiometric neutralization levels within experimental error (<5%).

Thermal Analysis. Glass transition temperatures (T_g) were determined using a TA Instruments Q2000 differential scanning calorimeter (DSC). The response was measured over the temperature range of 40 to

Received: April 27, 2011

Revised: June 5, 2011

Published: June 20, 2011

Table 1. Neutralization Levels, Degrees of Sulfonation and Neutralizing Ion Types Investigated

% sulfonation	% neutralization				
	0	25	50	75	100
3.5	H		Zn, Na, Cs		Zn, Na, Cs
6.7	H		Zn, Na, Cs		Zn, Na, Cs
9.5	H	Zn	Zn, Na, Cs	Zn	Zn, Na, Cs

180 °C at a heating rate of 10 °C/min under a nitrogen flow of 50 mL/min. The T_g was taken as the inflection point in the DSC thermogram from the second heating scan.

Scanning Transmission Electron Microscopy. STEM specimens were sectioned from the solvent-cast, dried, and annealed ionomer films at room temperature using a Reichert-Jung ultramicrotome with a diamond knife to a nominal thickness of 30–50 nm. STEM experiments were performed using a JEOL 2010F field emission scanning transmission electron microscope. High-angle annular dark field (HAADF) STEM images were recorded using a 0.7 nm STEM probe and a 70 μ m condenser aperture at an accelerating voltage of 200 keV.

X-ray Scattering. X-ray scattering experiments were performed with a multiangle X-ray scattering (MAXS) apparatus using Cu K_α X-rays generated from a Nonius FR 591 rotating-anode generator operated at 40 kV and 85 mA. The bright, highly collimated beam was obtained via Osmic Max-Flux optics and triple pinhole collimation under vacuum. The scattering data were collected using a Bruker Hi-Star multiwire detector with sample-to-detector distances of 11, 54, and 150 cm. *Dasqueeze* software was used to integrate the isotropic 2-D data into a 1D plot.¹⁴

The scattering data of the SPS ionomers was fit to:

$$I(q) = I_{KT}(q) + L_1(q) + L_2(q) + C \quad (1)$$

where $I_{KT}(q)$ is the scattering intensity defined by the Kinning–Thomas (K–T) modified hard-sphere model^{10,15} (see Supporting Information), $L_1(q)$ and $L_2(q)$ are Lorentzian functions used to fit the two polystyrene amorphous halos in the wide angle region, and C is a constant used to account for the instrumental background scattering, as previously reported.¹⁶ The scattering vector $q = 4\pi \sin(\theta)/\lambda$ where 2θ is the scattering angle and λ is the X-ray wavelength.

Dielectric Relaxation Spectroscopy. Isothermal relaxation spectra were collected on samples 0.2–0.4 mm thick in a parallel plate capacitor configuration using brass electrodes with a top electrode diameter of 20 mm. Isothermal spectra were collected under nitrogen using a Novocontrol GmbH Concept 40 BDRS spectrometer using a frequency range of 1 mHz to 10 MHz on heating from 10 to 220 °C.

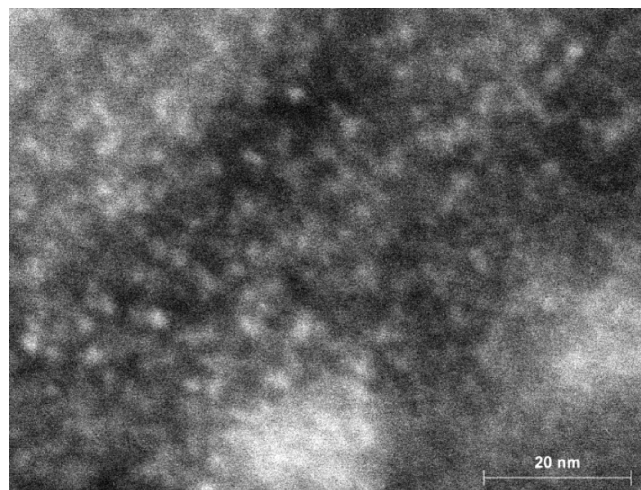
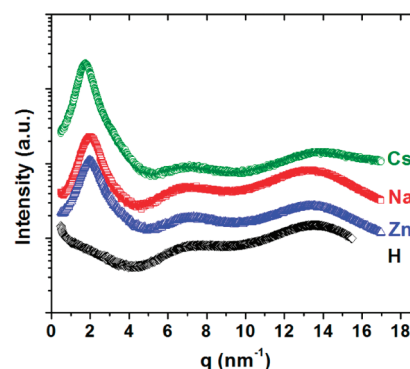
Dielectric strength ($\Delta\epsilon$) and characteristic relaxation time (τ_{HN}) were determined for each relaxation process by fitting the dielectric loss to the appropriate form of the Havriliak–Negami (HN) function^{17,18}

$$\epsilon''_{HN}(\omega) = \frac{\Delta\epsilon}{(1 + (i\tau_{HN}\omega)^a)^b} \quad (2)$$

where a and b are shape parameters. The characteristic relaxation time is related to the frequency of maximum loss (f_{\max}) by

$$f_{\max} = \left[\frac{1}{2\pi\tau_{HN}} \right] \left[\frac{\sin(\pi a/(2+2b))}{\sin(\pi ab/(2+2b))} \right]^{1/a} \quad (3)$$

Above T_g , the contribution from ohmic conduction dominates the loss contribution (ϵ''), potentially masking dipolar processes. The “conduction free” dielectric loss was determined using the derivative method described in our previous papers.^{12,13}

**Figure 1.** Representative HAADF STEM image of SPS9.5–100%Cs.**Figure 2.** Representative X-ray scattering intensity vs scattering vector q for SPS9.5–100%H (black diamonds), Zn (blue triangles), Na (red squares), and Cs (green circles).

RESULTS AND DISCUSSION

Morphology. Spherical bright regions corresponding to Cs-rich ionic aggregates within a PS matrix of lower average atomic number are observed in HAADF STEM images of the Cs-neutralized SPS ionomers (Figure 1). The diameters of the aggregates were determined by the full width at half-maximum (fwhm) of the Gaussian functions fit to the intensity profiles taken across individual bright features.¹⁹ Taking into account the extensive projection overlap in the STEM images and the limit of instrumental resolution, STEM images indicate that the diameters of Cs ionic aggregates are ~ 2 nm and are independent of sulfonation level. The size of the Zn aggregates, as previously published, were ~ 2 nm from STEM as well.¹³ For the Na-neutralized ionomers there is insufficient contrast between the aggregates and matrix, therefore aggregate sizes are determined by fitting the scattering data to the K–T modified hard sphere model.

Representative scattering profiles for the SPS9.5–100%H, Zn, Na, and Cs are shown in Figure 2. Three isotropic maxima are observed: the polystyrene amorphous halo (~ 13 nm^{−1}), the polystyrene “polymerization peak” (~ 7 nm^{−1}),²⁰ and the aggregate peak (1 – 2 nm^{−1}). The K–T modified hard sphere model was used to facilitate the interpretation of the aggregate peak. The model assumes that this peak arises from interparticle scattering from monodisperse, spherical aggregates homogeneously

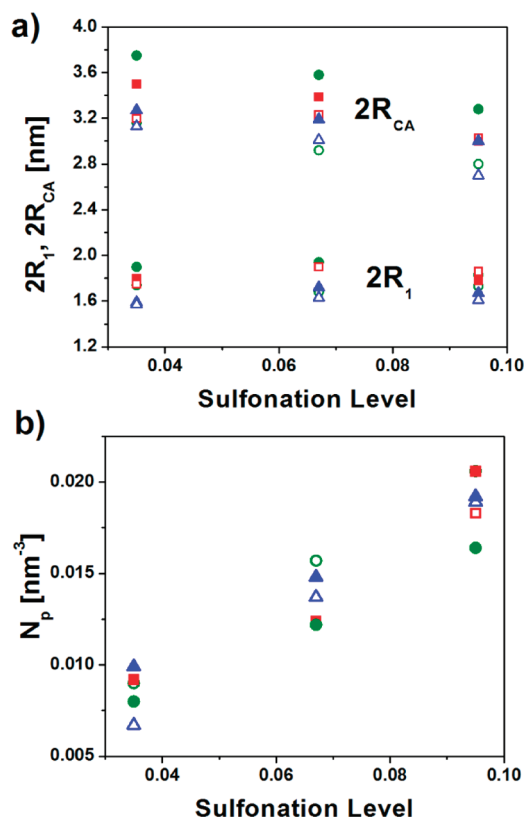


Figure 3. (a) $2R_1$ and $2R_{CA}$ and (b) N_p for all sulfonation levels neutralized with Cs (green circles), Na (red squares), and Zn (blue triangles) at 50 (open symbols) and 100% (filled symbols).

distributed in the polymer matrix of lower electron density. Four variable parameters are utilized to characterize aggregation: the aggregate radius R_1 , the radius of closest approach R_{CA} , the number density of the aggregates N_p , and the amplitude A of the scattering maxima.¹⁰ The parameters $2R_1$, $2R_{CA}$, and N_p are shown in Figure 3a and b as a function of sulfonation level for 50 and 100% Na, Cs, and Zn.

Na, Cs, and Zn aggregate diameters ($2R_1$) are approximately independent of sulfonation and neutralization, while R_{CA} decreases slightly, and the number density of ionic aggregates (N_p) increases with increasing sulfonation (Figure 3, parts a and b). In studies of Cu(II)-neutralized poly(styrene-*co*-methacrylic acid) (Cu-SMAA) ionomers²¹ and Zn-neutralized poly(ethylene-*co*-methacrylic acid) (Zn-EMAA)^{22,23} the aggregate diameter (~ 1.5 nm for Cu-SMAA²¹ and ~ 2.5 – 2.8 nm for Zn-EMAA²²) is similarly independent of neutralization level and acid content. This suggests that ionic aggregate size is largely dictated by the chemistry of the polymer backbone and the covalently bound counterion. Previous findings by Zhou et al. showed that there is a weak correlation between the size of ionic aggregates and the radius of neutralizing cations in SPS1.9–12.5%M ($M = \text{Na}, \text{Cs}, \text{Cu}, \text{Mg}, \text{Zn}, \text{Ba}$).¹⁰ We generally observe a very slight increase in aggregate size with increasing ionic radii (ionic radii for Zn^{2+} , Na^+ , and Cs^+ are 74, 102, and 167 pm, respectively²⁴), however, particularly at higher sulfonation levels, this difference is not significant.

The chain segments tethered to the aggregate by their anion experience reduced conformational mobility in the so-called “region of restricted mobility”, theorized by Eisenberg et al.^{4,25,26} Eisenberg et al. estimated the length scale of the region of restricted mobility to

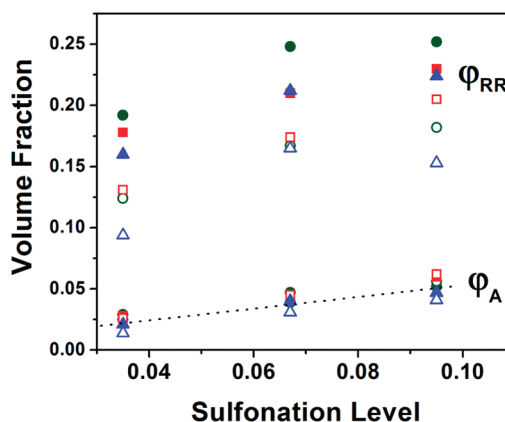


Figure 4. Volume fraction of restricted regions and aggregates for three sulfonation levels, neutralized with Cs (green circles), Na (red squares), and Zn (blue triangles) at 50 (open symbols) and 100% (filled symbols). A dotted line is drawn to guide the eye through the aggregate volume fraction values.

be on the order of the persistence length of the polymer chain (~ 1 nm for PS),²⁵ which is on the order of $R_{CA} - R_1$. The volume fractions of the region of restricted mobility (ϕ_{RR}) and aggregates (ϕ_A) can be estimated using R_1 , R_{CA} , and N_p :

$$\phi_{RR} = \frac{4}{3}\pi(R_{CA}^3 - R_1^3)N_p \quad (4)$$

$$\phi_A = \frac{4}{3}\pi R_1^3 N_p \quad (5)$$

ϕ_{RR} and ϕ_A are shown in Figure 4 as a function of sulfonation level for 50 and 100% Na, Cs, and Zn. The volume fraction of the aggregates increases only slightly with increasing sulfonation level but, surprisingly, is not strongly affected by the neutralizing ion, despite the larger ionic radius of Cs. The volume fraction of the restricted region increases slightly with increasing sulfonation and neutralization.

Segmental Dynamics. The segmental relaxation (α) arises from cooperative motion of chain segments and is related to the glass transition. In our previous papers we observed that this relaxation is slowed by the addition of sulfonic acid groups and that two segmental relaxations, α and α_2 , are present in the Zn-neutralized ionomers, corresponding to the motion of chain segments in the matrix and those restricted by the presence of the aggregate, respectively.^{12,13} In the following sections, we will discuss the role of ion type, percent sulfonation and degree of neutralization on segmental motion.

Cation Effects On Segmental Dynamics. The relaxation breadth, time and strength of the segmental relaxations of SPS ionomers is highly dependent on counterion type (Figure 5). While the Zn-neutralized form exhibits two relaxations, the Na- and Cs-neutralized ionomers exhibit a single but very broad (6–7 decades in frequency) segmental relaxation (Figure 5, parts a and b).

It is important to note that the strength of the segmental relaxation arises primarily from chain segments with acid or ionic functionality ($-\text{SO}_3\text{H}$ and $-\text{SO}_3\text{M}$ groups). For SPS Zn ionomers the presence of α and α_2 indicate two distinct relaxing environments corresponding to fast and slow segmental motion associated with chain segments in the matrix and close to the ionic aggregates, respectively. The segmental relaxations of the

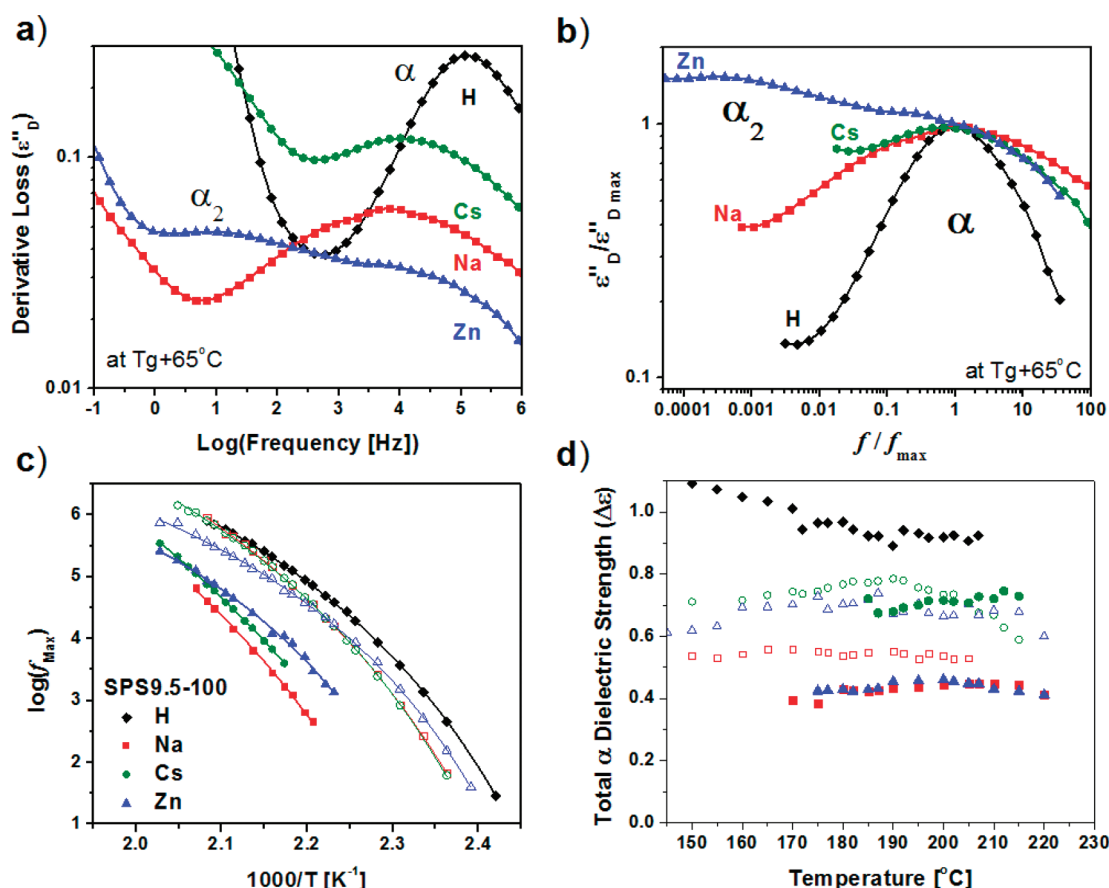


Figure 5. (a) Derivative loss spectra and (b) derivative loss spectra normalized by the maximum loss and relaxation frequency (lines are to guide the eye) for SPS-9.5 100%M, where M is designated in the figure. Temperature dependence of (c) relaxation frequency (lines are fits to the VFT equation) and (d) dielectric strength of α for SPS-9.5 H (diamonds), Na (squares), Cs (circles) and $\alpha + \alpha_2$ for Zn (triangles) at 50% (open symbols) and 100% neutralization (solid symbols).

Zn ionomer together span more than 7 decades in frequency. For SPS Na and Cs ionomers, however, the relaxing environment is diffuse with a single broad process also spanning 6–7 decades in frequency. This distinction likely results from the divalent nature of the Zn cations that slows the chains in the regions of restricted mobility more significantly than monovalent cations by directly cross-linking chains.

The maximum relaxation frequency and total dielectric strength of the α process (Figure 5, parts c and d, respectively) are also influenced by ion type as well as degree of neutralization, which was discussed extensively for SPS Zn in our recent publication.¹³ The relaxation frequency follows a VFT temperature dependence:

$$f_{\max} = f_0 \exp\left(\frac{B}{T - T_0}\right) \quad (6)$$

where T_0 is the Vogel temperature, f_0 is associated with vibration lifetimes²⁷ and the temperature coefficient B is related to the apparent activation energy ($E_a = BR/(1 - T_0/T)^2$).²⁸ The dynamic T_g (T_{ref}) is determined by extrapolating the VFT fit to $\tau = 100$ s ($f = 0.00159$ Hz). T_{ref} for the α process is generally within error of the calorimetric T_g . See Supporting Information, Table S1.

Role of Degree of Neutralization on Segmental Dynamics. The dielectric strength is related to both the number density of

dipoles and their dipole moments by the Onsager equation:^{12,29}

$$\Delta\epsilon = \frac{1}{3\epsilon_0} \left(\frac{\epsilon_s(\epsilon_\infty + 2)^2}{3(2\epsilon_s + \epsilon_\infty)} \right) g \frac{\mu^2 N}{kT V} \quad (7)$$

where g is the Kirkwood–Fröhlich correlation factor which takes into account the orientational effects of short-range interactions between molecules ($g = \mu_{\text{eff}}^2 / \mu_o^2$, μ_{eff} and μ_o are the condensed and gas phase dipole moments, respectively),³⁰ N/V is the number density of sulfonic acid and sulfonate–ion groups, ϵ_s and ϵ_∞ are the low and high frequency limits of the dielectric constant, and ϵ_0 is the vacuum permittivity. For the acid copolymer precursors of these ionomers we determined the ideal dielectric strength of the segmental relaxation for the limiting case where all dipoles are contributing freely. From these calculations, we concluded that the experimental dielectric strength (~ 1 for SPS9.5–100H) is reduced from the limiting case (~ 2.5) by net antiparallel interactions, namely the acid groups are associated with one another and thereby reduce the dielectric strength.¹²

$\Delta\epsilon_\alpha$ for the neutralized ionomers (Figure 5d) are clearly reduced from the acid form. If all acid groups were contributing freely to the dielectric strength at 50% neutralization we would expect $\Delta\epsilon_\alpha$ ($\Delta\epsilon_{\alpha+\alpha_2}$ for Zn) to be at least 1 for SPS9.5–50M, not including contributions from the 50% ionic species if all of the sulfonic acid groups are free to contribute to the dielectric

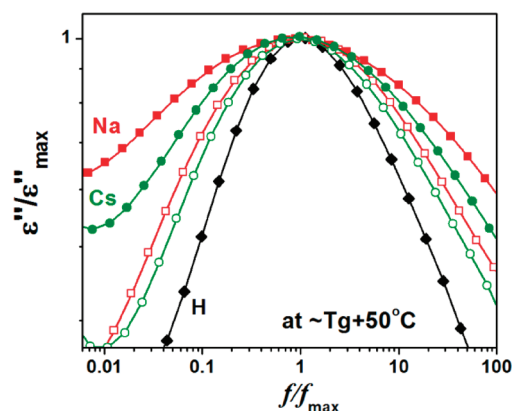


Figure 6. Neutralization effect on the segmental process for SPS6.7-*y*Na (squares) and Cs (circles) at 0% (diamonds), 50% (open symbols), and 100% (filled symbols) neutralization.

strength of the segmental process.¹² The experimental strength, however, is just ~ 0.5 for Na ionomers and 0.7 for the Cs and Zn ionomers. This discrepancy between the expected and measured values is likely due to a reduction in effective dipole moment arising from unneutralized acid groups participating in ionic aggregates.

At 100% neutralization we expect all of the sulfonate moieties to participate in the ionic aggregates, reducing their effective dipole moment due to dipolar cancellation. Therefore, upon full neutralization, associations of the ionic groups are expected to decrease $\Delta\epsilon_\alpha$ significantly, however, this is clearly not the case. The total segmental relaxation strength decreases from 0.5 to 0.4 for Na and from 0.7 to 0.4 for Zn after complete neutralization, but that for the Cs-neutralized ionomer remains constant (at ~ 0.7); all of which are significantly higher than that of PS (0.03). There are several possible sources for this unexpectedly high strength, including ionic groups sterically excluded from the aggregates and a small fraction of residual unneutralized acid groups in the matrix. In addition, as previously discussed for Zn-neutralized ionomers, it is likely that localized motion of the sulfonate-ion groups within the aggregate contributes to the strength of the segmental motion of slow chain segments near the aggregates.¹³ The significantly higher strength of the Cs-neutralized ionomer, in addition to a higher dipole moment, is likely due to ionic group exclusion from the aggregate due to the bulky and weaker binding nature of the Cs ion. The dipole moments for benzene-sulfonate coordinated with Li^+ , Na^+ , and K^+ from *ab initio* calculations are 5.7 , 7.8 , and 9.8 D, respectively.³¹ Because of the number of electrons in Cs^+ the same basis set could not be used. However, since Li, Na, K, and Cs are all alkali metals, a first order approximation of the dipole moment would be about 14 D for benzene-sulfonate coordinated with Cs.

In addition to a decrease in f_{max} , neutralization also has a significant effect on the shape of the segmental processes. As noted earlier, the ionomers containing monovalent Na and Cs do not exhibit a distinct slow α_2 process, but there is a clear broadening effect of segmental process as the ionomer is neutralized. This is shown at 6.7% sulfonation as a representative example in Figure 6. This broadening is rather symmetric and is more pronounced for SPS neutralized with Na than Cs, likely due to the higher binding energy of the Na^+ compared to Cs^+ . A similar increase in broadening and slowing of the α relaxation time and increase in symmetry is also observed with increasing crystallization of semicrystalline polymers.^{32,33} The mobility restriction on chain dynamics imposed

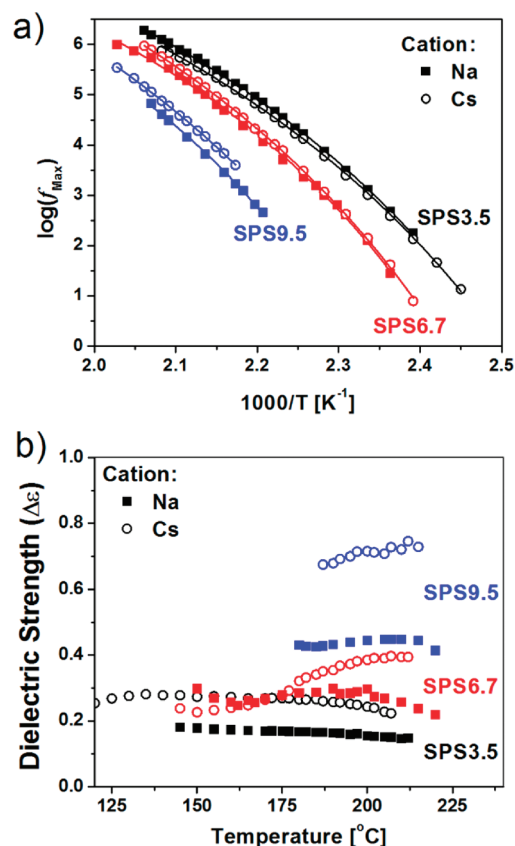


Figure 7. (a) Segmental relaxation frequency maxima and b) dielectric strength for SPS3.5 (black symbols), 6.7 (red symbols), and 9.5 (blue symbols) neutralized with Cs (open circles) and Na (closed squares) at 100% neutralization.

by the ionic aggregates is comparable to the restrictions imposed by crystalline regions.

Sulfonation Effects for Na- and Cs-Neutralized SPS. The relaxation time of the segmental process slows systematically with increasing sulfonation level for the neutralized ionomers (Figure 7a) and is not strongly dependent on ion type for Na- and Cs-neutralized SPS. This is consistent with an increase in number density of the ionic aggregates (Figure 3b) which physically cross-link the polymer. As the number of cross-links increases the segmental mobility is systematically reduced. This effect is expected and has been observed in chemically cross-linked polymers.^{34–36} Additionally, the breadth of the segmental relaxation also increases slightly with sulfonation (see Supporting Information, Figure S2).

The dielectric strength of the segmental process generally increases with increasing sulfonation and does not have a significant temperature dependence. For the Na-neutralized ionomers $\Delta\epsilon$ increases from ~ 0.2 to 0.4 for 100% Na (Figure 7b) and from ~ 0.2 to 0.6 for 50% Na (not shown) as the sulfonation level increase from 3.5 to 9.5 mol %. The strength of the Cs ionomers is slightly higher (~ 0.3 – 0.7 at 100% Cs, Figure 7b, and ~ 0.3 – 0.8 at 50% neutralization) over the same sulfonation range. At 100% Cs neutralization, an increase in $\Delta\epsilon$ with temperature is observed at the higher sulfonation levels, which suggests that some ionic groups are released from the aggregates and are free to contribute to the strength of this process at higher temperatures for the fully Cs-neutralized ionomers.

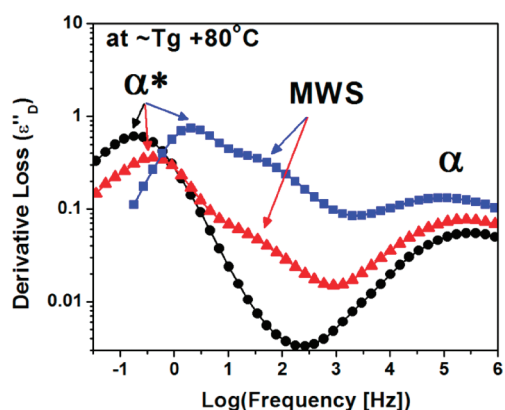


Figure 8. Conduction free dielectric loss vs frequency for 100% Cs-neutralized SPS ionomers at 3.5 (black circles), 6.7 (red triangles), and 9.5% (blue squares) sulfonation.

High Temperature Relaxation Processes. The high temperature relaxation phenomena for the neutralized ionomers, revealed after removal of the conductivity contribution, is distinct for each ion type. For the acid copolymers, two relaxations due to Maxwell–Wagner Sillars (MWS) interfacial polarization and association/dissociation dynamics of hydrogen bonds (α^*) were observed.¹² A single high temperature relaxation, attributed to MWS interfacial polarization, was observed for the Zn-neutralized ionomers, which shifted with increasing neutralization to lower frequencies.¹³

For 50% Na-neutralized SPS, two relaxation processes are also observed at similar frequencies and temperatures as the relaxations in the acid form, and very likely have the same origin. At 100% Na neutralization no high temperature relaxations are observed – likely because they are shifted to lower frequencies and higher temperatures than our measured experimental range (see Supporting Information, Figure S3).

For 100% Cs-neutralized ionomers two overlapping relaxations are evident at 6.7 and 9.5% sulfonation (Figure 8). The strength of these processes is too low for electrode polarization to be a possible origin. The relaxation at intermediate frequencies, roughly 4 decades slower than the α process, is observed for SPS6.7 and 9.5–100Cs (Figure 8) and shifts to higher frequencies and increases in strength with degree of sulfonation (0.1 to 1 for SPS6.7 and SPS9.5–100Cs, respectively; data not shown) corresponding with an increase in aggregate number density (Figure 3b). Maxwell–Wagner Sillars interfacial polarization is the likely origin for this process, as it corresponds with the dc conductivity plateau and follows a similar temperature dependence. However, due to the limited number of temperatures at which this process is visible and the uncertainty in fitting, definite assignment is not possible.

The stronger lower frequency relaxation process observed in the Cs ionomers (5–6 decades lower in frequency than α) follows an Arrhenius temperature dependence in the temperature range it is observed in and is only slightly dependent on neutralization and sulfonation levels (Figure 9a). MWS is an unlikely origin of this process, as previous findings for unneutralized and Zn-neutralized SPS revealed that the MWS relaxation frequency was dependent on sulfonation and neutralization and had a VFT temperature dependence.^{12,13} This process likely arises from interaggregate ion hopping, analogous to hydrogen bond association/disassociation dynamics (α^*). This is supported

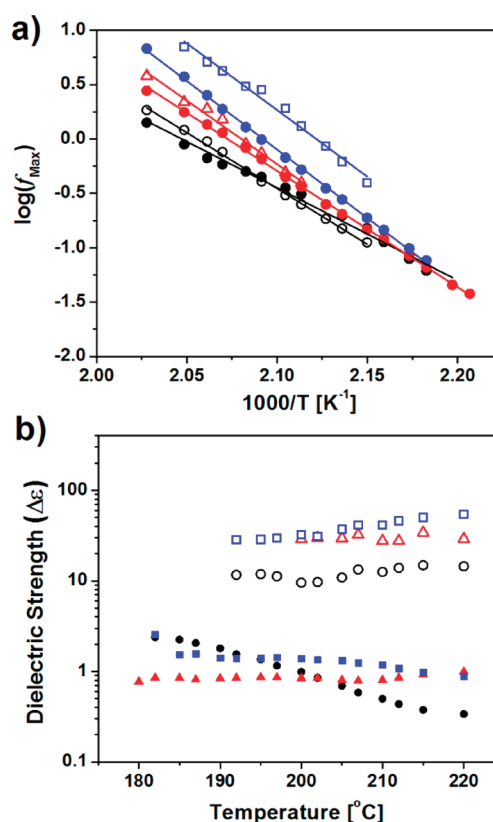


Figure 9. (a) Relaxation frequency fit to the Arrhenius equation (solid lines) and (b) dielectric strength of the α^* process for SPS3.5 (black circles), 6.7 (red triangles), and 9.5 (blue squares) neutralized with Cs at 50% (open symbols) and 100% (filled symbols).

by the activation energies of this process, 160 to 240 kJ/mol, which are in the range of the ion hopping activation energy measured from rheology experiments by Eisenberg et al. for Na-neutralized SPS.⁴ The activation energy of this process increases with increasing sulfonation, consistent with the observation by Eisenberg et al.⁴ and is likely associated with the increase in T_g .

The relaxation frequency and strength of this process was found to increase slightly with increasing sulfonation (Figure 9, parts a and b). Increasing the neutralization level from 50 to 100% Cs, however, decreased the relaxation frequency slightly and lowered the strength by roughly an order of magnitude (Figure 9, parts a and b). At 50% neutralization there is likely a strong contribution to the strength of this process from association dynamics of hydrogen bonded acid groups as is observed in the acid copolymers and is discussed in a previous publication.¹²

SUMMARY

The morphology and dynamics SPS ionomers neutralized with Na, Cs and Zn cations were investigated using STEM, X-ray scattering and dielectric relaxation spectroscopy. Ionic aggregates size (~ 2 nm in diameter) was found to be independent of the extent of sulfonation and degree of neutralization and was not strongly influenced by ionic radius. The volume fraction of the aggregates and restricted region, determined from the K–T fit parameters R_1 , R_{CA} , and N_p , were found to increase with increasing sulfonation.

SPS ionomers neutralized with monovalent Na and Cs cations exhibit one very broad segmental process with relaxation times

and strengths are highly dependent on degree of sulfonation and neutralization, whereas Zn-neutralized SPS exhibited two distinct segmental processes due to the direct cross-linking effect of the divalent ion. Increasing neutralization from 50 to 100% results in a slowing down of the segmental relaxation time and an increase in relaxation breadth. In addition, the segmental process slowed systematically with increasing sulfonation due to the increased number density of aggregates acting as physical cross-links.

At high temperatures, the derivative formalism facilitated observation of two high temperature relaxations for fully neutralized Cs ionomers. These relaxations likely arise from Maxwell–Wagner–Sillars interfacial polarization and ionic association/disassociation dynamics likely arising from interaggregate ion hopping. The high temperature relaxation phenomena for fully Na-neutralized SPS were shifted out of the observed temperature/frequency window – likely due to the higher binding energy of the Na ion.

■ ASSOCIATED CONTENT

S Supporting Information. The Kinning–Thomas modified hard-sphere model, the dynamic glass transition temperature, segmental process breadth as a function of degree of sulfonation, and high temperature relaxations. This material is available free of charge via the Internet at <http://pubs.acs.org>.

■ AUTHOR INFORMATION

Present Addresses

⁵The Dow Chemical Company, Springhouse, PA 19477.

■ ACKNOWLEDGMENT

This research was supported by the U.S. Department of Energy, Office of Basic Energy Sciences, Division of Materials Sciences and Engineering, under Award DEFG02-07ER46409. We would also like to thank Wenjuan Liu for her contribution and helpful discussion. The X-ray scattering facility at the University of Pennsylvania is supported in part by the National Science Foundation, MRSEC-DMR05-20020.

■ REFERENCES

- (1) Grady, B. P. *Polym. Eng. Sci.* **2008**, 48 (6), 1029–1051.
- (2) Weiss, R. A.; Fitzgerald, J. J.; Kim, D. *Macromolecules* **1991**, 24 (5), 1071–1076.
- (3) Weiss, R. A.; Yu, W. C. *Macromolecules* **2007**, 40 (10), 3640–3643.
- (4) Hird, B.; Eisenberg, A. *Macromolecules* **1992**, 25 (24), 6466–6474.
- (5) Colby, R. H.; Zheng, X.; Rafailovich, M. H.; Sokolov, J.; Peiffer, D. G.; Schwarz, S. A.; Strzhemechny, Y.; Nguyen, D. *Phys. Rev. Lett.* **1998**, 81 (18), 3876.
- (6) Earnest, T. R.; Higgins, J. S.; Handlin, D. L.; MacKnight, W. J. *Macromolecules* **1981**, 14 (1), 192–196.
- (7) Yarusso, D. J.; Cooper, S. L. *Macromolecules* **1983**, 16 (12), 1871–1880.
- (8) Weiss, R. A.; Lefelar, J. A. *Polymer* **1986**, 27 (1), 3–10.
- (9) Ding, Y. S.; Hubbard, S. R.; Hodgson, K. O.; Register, R. A.; Cooper, S. L. *Macromolecules* **1988**, 21 (6), 1698–1703.
- (10) Zhou, N. C.; Chan, C. D.; Winey, K. I. *Macromolecules* **2008**, 41 (16), 6134–6140.
- (11) Li, C.; Register, R. A.; Cooper, S. L. *Polymer* **1989**, 30 (7), 1227–1233.
- (12) Castagna, A.; Wang, W.; Winey, K. I.; Runt, J. *Macromolecules* **2010**, 43 (24), 10498–10504.
- (13) Castagna, A.; Wang, W.; Winey, K. I.; Runt, J. *Macromolecules* **2011** in press.
- (14) Heiney, P. A. *Commission on Powder Diffraction Newsletter* **2005**, 32, 9–11.
- (15) Kinning, D. J.; Thomas, E. L. *Macromolecules* **1984**, 17, 1712–1718.
- (16) Benetatos, N. M.; Heiney, P. A.; Winey, K. I. *Macromolecules* **2006**, 39 (16), 5174–5176.
- (17) Havriliak, S.; Negami, S. *Polymer* **1967**, 8 (4), 161–210.
- (18) Wubbenhorst, M.; van Turnhout, J. J. *Non-Cryst. Solids* **2002**, 305 (1–3), 40–49.
- (19) Benetatos, N. M.; Heiney, P. A.; Winey, K. I. *Macromolecules* **2006**, 39 (16), 5174–5176.
- (20) Ayyagari, C.; Bedrov, D.; Smith, G. D. *Macromolecules* **2000**, 33 (16), 6194–6199.
- (21) Wang, W.; Chan, T.-T.; Perkowski, A. J.; Schlick, S.; Winey, K. I. *Polymer* **2009**, 50 (5), 1281–1287.
- (22) Laurer, J. H.; Winey, K. I. *Macromolecules* **1998**, 31 (25), 9106–9108.
- (23) Seitz, M. E.; Chan, C. D.; Oppen, K. L.; Baughman, T. W.; Wagener, K. B.; Winey, K. I. *J. Am. Chem. Soc.* **2010**, 132 (23), 8165–8174.
- (24) Speight, J. G., *Lange's Handbook of Chemistry*; McGraw-Hill: New York: 2005.
- (25) Eisenberg, A.; Hird, B.; Moore, R. B. *Macromolecules* **1990**, 23 (18), 4098–4107.
- (26) Eisenberg, A.; Kim, J.-S., *Introduction to Ionomers*; Wiley: New York, 1998.
- (27) Santangelo, P. G.; Roland, C. M. *Macromolecules* **1998**, 31 (14), 4581–4585.
- (28) van Turnhout, J.; Wubbenhorst, M. J. *Non-Cryst. Solids* **2002**, 305 (1–3), 50–58.
- (29) Kremer, F.; Schonhals, A., *Broadband Dielectric Spectroscopy*; Springer-Verlag: Berlin, 2003.
- (30) Alexandrovich, P. S.; Karasz, F. E.; MacKnight, W. J. *J. Macromol. Sci., Part B* **1980**, 17 (3), 501–516.
- (31) Liu, W. Unpublished Results; Castagna, A., Ed.; State College, PA, 2010.
- (32) Ezquerra, T. A.; Baltà-Calleja, F. J.; Zachmann, H. G. *Polymer* **1994**, 35 (12), 2600–2606.
- (33) Ezquerra, T. A.; Liu, F.; Boyd, R. H.; Hsiao, B. S. *Polymer* **1997**, 38 (23), 5793–5800.
- (34) Kramarenko, V. Y.; Ezquerra, T. A.; Sics, I.; Baltà-Calleja, F. J.; Privalko, V. P. *J. Chem. Phys.* **2000**, 113 (1), 447–452.
- (35) Glatz-Reichenbach, J. K. W.; Sorriero, L.; Fitzgerald, J. J. *Macromolecules* **1994**, 27 (6), 1338–1343.
- (36) Roland, C. M. *Macromolecules* **1994**, 27 (15), 4242–4247.